

## Article

# Power Consumption Influence Test of Castor Disc-Cutting Device

Teng Wu, Fanting Kong \*, Lei Shi, Qing Xie, Yongfei Sun and Changlin Chen

Nanjing Research Institute for Agricultural Mechanization, Ministry of Agriculture, Nanjing 210014, China

\* Correspondence: kongfanting@caas.cn; Tel.: +86-153-6609-2846

**Abstract:** This study theoretically analyzed the cutting process of castor and determined the structural parameters of the key component of the castor disc-cutting device, aiming to obtain the optimal operation parameter combination and reduce the cutting resistance and power consumption during the harvesting process. The effects of the cutting-disc thickness, cutting-disc rotational speed, feeding speed, and edge angle on the cutting power consumption were studied using an orthogonal rotation combination experiment. The response surface method was used to optimize the parameters, and the mathematical relationship model between the cutting power consumption and each factor was established to determine the optimal parameter combination for disc cutting. The simulation results showed that the optimal combination of cutting parameters was cutting-disc thickness of 3 mm, cutting-disc rotational speed of 550 r/min, feeding speed of 0.6 m/s, and edge angle of 20°. Under these conditions, the cutting power consumption was 1.20375 J. The test results were basically consistent with the model prediction results. Therefore, this study provided a theoretical basis and reference for the design and improvement of castor harvesters.

**Keywords:** agricultural machinery; castor; theoretical analysis; power consumption; parameter optimization



**Citation:** Wu, T.; Kong, F.; Shi, L.; Xie, Q.; Sun, Y.; Chen, C. Power Consumption Influence Test of Castor Disc-Cutting Device. *Agriculture* **2022**, *12*, 1535. <https://doi.org/10.3390/agriculture12101535>

Academic Editors: Zhichao Hu and Fengwei Gu

Received: 11 August 2022

Accepted: 19 September 2022

Published: 23 September 2022

**Publisher's Note:** MDPI stays neutral with regard to jurisdictional claims in published maps and institutional affiliations.



**Copyright:** © 2022 by the authors. Licensee MDPI, Basel, Switzerland. This article is an open access article distributed under the terms and conditions of the Creative Commons Attribution (CC BY) license (<https://creativecommons.org/licenses/by/4.0/>).

## 1. Introduction

Castor oil, as an important chemical and strategic raw material [1], is widely used in the aviation industry, the chemical industry, automobiles, fragrances, and medicine. Moreover, it is a kind of industrial vegetable oil source with comprehensive development potential [2–4]. With the development of new technologies and processes in the petrochemical industry, the demand for castor oil is expected to grow. Therefore, in order to expand the planting areas for castor in China and improve the yield of castor, it is urgent to realize the mechanization of the production of castor harvesting.

At present, there is no mature castor harvest equipment in castor production, and castor harvesting is performed manually in China [5–7]. The current castor industry urgently needs a castor harvester with low harvest loss and high work efficiency. Several castor-harvesting machines have been developed by foreign companies. A full feeding castor harvester was developed by the German CLAAS company [8]; it has a high degree of mechanization, but also high rates of leakage and damage. The vibrating castor harvester designed by DEERE Company [9] of the United States has a low net harvesting rate when the water content is high. The comb-type castor-picking device was designed by Li et al. [10] in China. It uses the clamping effect of two adjacent teeth to separate the castor from the stalk under the rotating movement of the picker to complete the picking. However, it has difficulty in picking dwarf castor with low panicle heights. The castor harvester developed by Wu et al. [11] cuts the castor stalk with a cutting knife and then pulls the plant out of the roller to complete the harvest of the castor. However, the net harvesting rate is only 67.1%, and the harvest effect needs to be improved. The 4BZ-4 self-propelled castor harvester developed by Wu et al. [12] uses the brush rollers to comb the castor capsule from the stem to complete the harvest; nevertheless, it is mainly suitable for the harvest of tall stalk castor. The castor harvester with double spring teeth was developed by Bai et al. [13] on the basis

of an existing agricultural harvester. The mathematical models between the cutting speed, and the forward speed effected on the cutting efficiency, were obtained, and a set of optimal cutter operating parameters were determined.

Song et al. [14] explore the effect of the knife section structural parameters as well as the operating parameters on the cutting efficiency rate of the cotton stalk reciprocating cutter, and optimize the structural parameters of the knife section; the simulation test was performed with ADAMS software. Guo et al. [15] established a logarithmic spiral equation of blade line, designed a special equal sliding-cutting angle saw tooth blade for cane straw, finished cutting tests on mature tomato and eggplant vines in different moisture contents, and recorded the cutting power and times as the cutting time to analyze cutting power and cutting efficiency. Chen et al. [16] studied the tensile and shearing characteristics of rind of corn stalk via quadratic orthogonal rotatory combination design. The results of a data analysis reveal that the shearing speed and moisture content are significant factors in the shear strength of rind of corn stalk, while the sampling height is not significant.

Castor harvesting is the interaction between the key components of castor fruit-picking equipment and the castor stalk. The harvesting process involves complex mechanisms and mutual mechanics. Existing research mostly addresses the physical properties and mechanical parameters of castor fruit; systematic research and optimization of the parameters of the castor harvesting operation is rare. At the same time, there is less research on the key components and the force analysis of the castor stalk in the process of castor harvesting. Consequently, the lack of research of castor stalks and the key parameters of harvesting operations has led to slow improvement in castor harvesting machinery, which has caused a fatal blow to the development of the Chinese castor industry. Therefore, improvement of the harvesting quality of the castor-picking device is an urgent issue.

Accordingly, a cutting-disc castor-picking device was designed according to the biological characteristics of low-growing castor in China. In order to improve the efficiency and reduce the power consumption of the operation, and explore the influencing factors of castor harvesting, a cutting-disc castor plant-picking test device was developed. The key structural parameters and operating parameters of the cutting-disc castor-picking mechanism were determined by combining theoretical analysis and experimental research. In this study, an orthogonal rotation combination multi-factor test was used to analyze the influences of the cutting-disc thickness, cutting-disc rotational speed, feeding speed, and edge angle for the power consumption. The aim was to reduce the cutting resistance and power consumption in the process of harvesting castor, based on the physical and mechanical characteristics of the stalk and the characteristics of the harvesting process [17–19], through an orthogonal rotation combination test. To provide reference for the research and optimization of the cutting castor-picking device, the structure and operation parameter combination for the cutting disc (the key component of the cutting castor-picking device) were optimized and verified by a bench test.

## 2. Materials and Methods

### 2.1. Mechanical Analysis of Cutting Process

The cutting process of a castor stalk is the result of the interaction between the stalk and cutting disc. Studying the force mode during the cutting process and clarifying the interaction relationship can provide a theoretical basis for analyzing the operation mechanisms of the stalk cutting and the design of the mechanism [20–22]. The main force for cutting the stalk is the cutting resistance. The force analysis is shown in Figure 1. The horizontal and vertical directions of the balance equation are as follows:

$$\begin{cases} F_a = F_c + F_e + F_{f1} + F_{f2} \cdot \cos \beta \\ F_b = F_d + F_{f2} \cdot \sin \beta \end{cases} \quad (1)$$

In the above,  $F_a$  is the horizontal component of the reaction force on the stem to the cutter head (N);  $F_e$  is the vertical component of the reaction force on the stem to the cutter head (N);  $F_c$  is the force of the stalk acting against the blade (N);  $F_{f1}$  is the friction of the

stalk against the blade (N);  $F_{f2}$  is the friction force of the stalk against the side edge of the cutting disc (N);  $\beta$  is edge angle ( $^{\circ}$ );  $F_b$  is the vertical component of the reaction force on the stem to the cutting disc (N); and  $F_d$  is the reaction force of the blade against the pressure of the stalk layer (N).

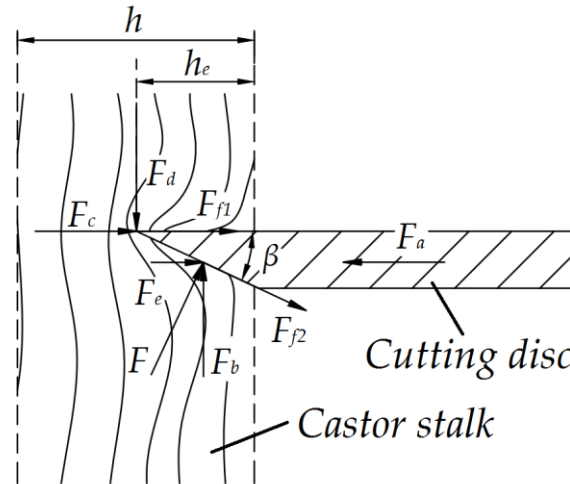


Figure 1. Schematic of Collision force and velocity of stalk.

$$F_c = \Delta l \sigma_c \tag{2}$$

Here,  $\Delta$  is the blade blunt width (m);  $l$  is the blade cutting length (m); and  $\sigma_c$  is the yield strength during cutting (MPa).

The reaction force  $F$  acting on the blade surface of the cutting disc is as follows:

$$F = F_e \cdot \sin \beta + F_b \cdot \cos \beta \tag{3}$$

In the above,  $F$  is the reaction force on the edge of the cutting disc (N).

It can be obtained from a geometric relation, as follows:

$$F_b = F \cdot \cos \beta \tag{4}$$

The side edge of the cutting disc friction force  $F_{f2}$  is calculated as follows:

$$F_{f2} = \mu F = \mu(F_e \cdot \sin \beta + F_b \cdot \cos \beta) \tag{5}$$

Here,  $\mu$  is the friction coefficient between the blade surface and stalk.

Its component force in the vertical direction is as follows:

$$F_{f1} = \mu_w F_d \tag{6}$$

In the above,  $\mu_w$  is the coefficient of friction in the stalk.

To analyze the relationship between  $F_e$  and  $F_d$ , it is necessary to discuss the element force on the blade surface. When the crop stalk group is squeezed, its stress and strain conform to Hooke's law; therefore, the stress–strain relationship of the stem squeezed by the outer edge is as follows:

$$\varepsilon = \frac{h_e}{h} = \frac{\sigma}{E} \tag{7}$$

Here,  $\varepsilon$  is the castor stalk cutting strain;  $h_e$  is the pressed thickness of castor stalks by the cutting edge (m);  $h$  is the cutting depth of the castor stalks (m);  $\sigma$  is the crushing stress (Pa); and  $E$  is the elastic modulus of the castor stalk (MPa);

When the depth of the blade deep into the stalk increases, the compression surface of the cutting disc increases as follows:

$$dF_x = ldh_e \cdot \tan \beta \quad (8)$$

According to Reznik hypothesized, a calculation can be made as follows:

$$\sigma = F_e / F \quad (9)$$

Then, the unit force acting on the plane of  $d_x$  of unit length  $L$  can be obtained using Equations (7) and (9).

$$dF_e = \sigma dx = E \epsilon dx = E \epsilon dh_e \cdot \tan \beta = E \frac{h_e}{h} dh_e \cdot \tan \beta \quad (10)$$

This is obtained by integrating the element forces, as follows:

$$F_e = \frac{E}{h} \tan \beta \int_0^{h_e} h_e dh_e = \frac{E}{2h} h_e^2 \tan \beta \quad (11)$$

In combination with Equations (1)–(6) and (11), the cutting force  $F_a$  on the length of the unit blade is as follows:

$$F_a = \Delta \sigma_c + \left[ \tan \beta + 2\mu \sin^2 \beta + \mu_w (1 - 2\mu \sin^2 \beta \cdot \tan \beta) \right] \frac{E}{2h} h_e^2 \quad (12)$$

According to the above theoretical analysis, the cutting resistance of the blade is related to the physical characteristics of the stalk, such as its elastic modulus and friction coefficient. Additionally, it is also related to the cutting-disc thickness, cutting-disc rotational speed, feeding speed, and edge angle. The cutting resistance and energy consumption of the cutting disc in the cutting process are the main parameters for power matching and optimization design of cutting-disc structure. In the cutting process of the cutting disc, suitable factors can be selected according to the theoretical analysis model to reduce cutting resistance and power consumption.

## 2.2. Test Materials

In this study, the castor cultivar was Israel Kaifeng No. 5 planted in Erlindai Village, Tumed Left Banner, Hohhot City, Inner Mongolia Autonomous Region. The seeds were sown by air suction planter in mid-April 2021.

In the middle of October 2021, physical characteristic parameters of mature castor plants were measured. The field sampling was conducted using the five-point method. Thirty castor plants were selected from each sampling point, and the parameter results were averaged. The main parameters of plants and field planting conditions are shown in Table 1. The main stalk diameter was the diameter at 15 mm above the ground, the average diameter of the main stalk was 21.4 mm, and the average height of the plant was 993.7 mm, as shown in Figure 2.

**Table 1.** Planting and plant characteristic parameters of castor.

Parameters	Values
Plant height/mm	890~1260
Yield/(kg·hm <sup>-2</sup> )	3187.5
Line spacing/mm	700
Row spacing/mm	550
Capsule number per plant	89~176
Minimum ear height/mm	211~459
Main stalk diameter/mm	19.8~24.9
Capsule diameter/mm	15.9~18.4



**Figure 2.** Castor stalk sample.

After the cutting test, the cut stalks were sealed and labeled with plastic wrap immediately. In accordance with EN ISO 6540-2010, a drying method was used to determine the moisture content of the test branches, and the sample mass was measured before drying (accurate to 0.001 g). After drying at  $103 \pm 2$  °C for 8 h, the mass was measured again. Subsequently, it was measured every 2 h; when the mass difference between the two measurements before and after did not exceed 0.002 g, the drying was regarded as completed, and the moisture content was to be calculated. The moisture content of the stalk was 12.5~20.8% during the experiment.

### 2.3. Test Equipment

#### 2.3.1. Cutting Structure Parameters

In accordance with the cutting type, the cutter was mainly divided into reciprocating and rotating. Based on the physical characteristics of the castor stalk, the cutting disc was selected to reduce the cutting resistance and reduce the loss rate caused by vibration. The cutting disc was divided into single disc and double disc according to the disk configuration. The feeding ability of the single cutting disc was poor, and it is generally only used in the harvester with clamping conveying and feeding. Therefore, the test bench designed in this study adopts the double cutting-disc mechanism.

In general, the structural parameters of the cutting disc were one of the key components affecting the cutting effect [23–25], and their structural parameters were mainly related to the physical parameters of the castor stalk. The structure of the cutting disc had an important influence on the cutting resistance, which was related to the shape and the effective arc length of the cutting edge. In order to increase the effective arc length and reduce the cutting resistance, this study designed a waved-type cutting disc in the early stage based on a preliminary test [26]. The diameter of the cutting disc was designed as 90 mm, and the horizontal distance of the center of the cutting disc was 10 mm. It is necessary to design the structural parameters of the waved-type cutting disc according to the physical characteristics of castor stalk. The structural parameters of the waved-type cutting disc are determined by the sliding angle in accordance with the calculation formula

of the distance between two points in the polar coordinate system (as shown in Figure 3). The polar equation of point  $m$  at the outer end of the cutting disc is as follows:

$$\rho^2 - 2\rho\rho_0 \cos(\theta - \theta_0) + \rho_0^2 = r^2 \tag{13}$$

where  $(\rho_0, \theta_0)$  is the center polar coordinates of an arc (mm,°);  $r$  is the radius of the waved arc (mm).  $\theta$  is the polar angle when the polar diameter is  $\rho$  (°).

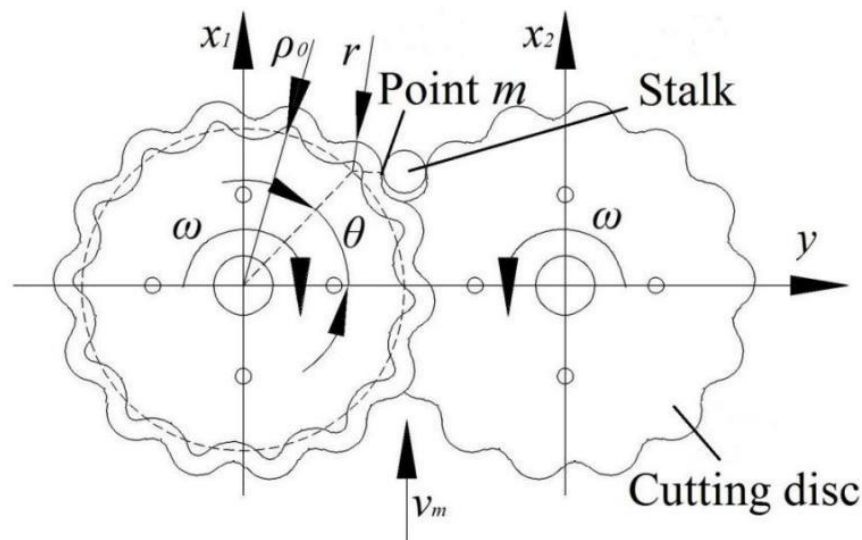


**Figure 3.** Structure of waved-type cutting disc. Point  $m$  is the cutting point of the stalk;  $v_m$  is the forward speed of the harvester ( $\text{m}\cdot\text{s}^{-1}$ );  $\omega$  is the cutting disc angular speed ( $\text{rad}\cdot\text{min}^{-1}$ ).

This can be obtained from Equation (13):

$$\rho = \rho_0 \cos(\theta - \theta_0) + \sqrt{r^2 - \rho_0^2 \sin^2(\theta - \theta_0)} \tag{14}$$

According to the geometrical relationship:

$$\tan \alpha = \rho / \rho' \tag{15}$$

Here,  $\alpha$  is the sliding cutting angle (°)

$$\rho' = \frac{d\rho}{d\theta} \tag{16}$$

Take the derivative of Equation (13):

$$\rho' = \frac{\rho\rho_0 \sin(\theta - \theta_0)}{\rho_0 \cos(\theta - \theta_0) - \rho} \tag{17}$$

In accordance with Equations (15) and (17), the sliding cutting angle can be obtained as follows:

$$\tan \alpha = \frac{\rho}{\frac{\rho\rho_0 \sin(\theta - \theta_0)}{\rho_0 \cos(\theta - \theta_0) - \rho}} = \cot(\theta - \theta_0) - \frac{\rho}{\rho_0 \sin(\theta - \theta_0)} \tag{18}$$

Substitute Equation (14) into Equation (18):

$$\alpha = \arctan \frac{\sqrt{r^2 - \rho_0^2 \sin^2(\theta - \theta_0)}}{-\rho_0 \sin(\theta - \theta_0)} \tag{19}$$

Due to maximum cutting resistance appearing after the cutting disc contacts the stalk, the polar angle  $\theta = 41.63^\circ$  was calculated according to the geometric relationship. The smaller the arc radius, the smaller the sliding angle. However, if arc radius was too small, the machining cost was high and the friction resistance would increase. When the sliding cutting angle was  $20^\circ \sim 55^\circ$ , it was beneficial to reduce the cutting power consumption. When the sliding cutting angle was  $41.52^\circ$ , it could be determined according to the actual situation and equation (19). The arc of the cutting disc was as follows: 14 sections of arc edge curves were arranged around the circumference, the radius of the arc was 10 mm, and the polar coordinates of the center of the arc were (80 mm,  $47^\circ$ ). The waved-type cutting disc designed based on the material characteristics of a castor stalk can give full play to the function of sliding cutting and clamping. The shear angle of the cutting disc was in dynamic change, and is not to be used as a factor for quantitative analysis.

According to the experimental statistics method: when the two-piece cutting-disc thickness was 2 mm, the edge angle was  $25^\circ$ ; when the two-piece cutting-disc thickness was 3 mm, the edge angle was  $20^\circ$ ; when the two-piece cutting-disc thickness was 3 mm, the edge angle was  $30^\circ$ ; when the two-piece cutting-disc thickness was 4 mm, the edge angle was  $15^\circ$ ; when the two-piece cutting-disc thickness was 4 mm, the edge angle was  $25^\circ$ ; when the two-piece cutting-disc thickness was 4 mm, the edge angle was  $35^\circ$ ; when the two-piece cutting-disc thickness was 5 mm, the edge angle was  $20^\circ$ ; when the two-piece cutting-disc thickness was 5 mm, the edge angle was  $30^\circ$ ; and when two-piece cutting-disc thickness was 6 mm, the edge angle was  $25^\circ$ ; a total of nine groups were produced. The cutting-disc material was 65 Mn. In the test, the factors of cutting-disc structure parameters were changed by changing different cutting-disc groups.

### 2.3.2. Test Bench Parameters

To test the actual operational performance of the double-disc cutting device, a castor stalk-cutting test bench was conducted at the Nanjing Institute of Agricultural Mechanization of the Ministry of Agriculture and Rural Affairs in July 2022, as shown in Figure 4.



**Figure 4.** Castor disc-cutting device. (1) Measuring and controlling system. (2) Cutting system. (3) Feeding system. (4) Power system.

In this test, two motors (driven by frequency conversion, modulating the rotational speed from 1 to 2000 r/min, rated power of 1.2 kW) provided power for the upper cutting disc and the bottom cutting disc, respectively. The power transmission drove a toothed chain (the toothed chain-driven sprocket and upper cutting disc were coaxial), and provided the upper cutting-disc rotational movement with chain movement. The torque sensor was fixed between the cutting disc and the rack to detect the torque during the cutting process. The bottom cutting disc was driven separately and directly connected to a torque sensor.

The cutting power consumption data measurement adopted a direct-connected torque sensor (Beijing New Aerospace Measurement and Control Technology Co., Ltd., model: JN338-A, measuring range 0~50 N·m, torque accuracy: 0.1~0.2% F·S). The data acquisition was performed using the UTD2101CEX digital storage oscilloscope with a frequency of 10 MHz and a dual-level low-pass filter. The castor sample was transported to the cutting disc device by the reducer motor (driven by frequency conversion and the rotational speed was modulated from 1 to 300 r/min with a rated power of 1.5 kW, corresponding to a feeding line speed from 0 to 2.0724 m/s). The cut plant was sent back to the rear by the toothed chain, thus completing the cutting process. Other auxiliary tools included vernier calipers, tape measures (0–150 m).

## 2.4. Experiment Design

### 2.4.1. Test Index

In general, the cutting resistance and power consumption of the cutting disc in the cutting process are the main parameters for power matching and optimizing the design of the cutting disc structure, and are of great significance to prolonging the tool life and improving the harvest working time.

For convenience in measurement and analysis, the power consumption of the unilateral cutting disc was used. The cutting power consumption  $W$  was obtained by integrating the torque measured by the torque sensor, as shown in Equation (20).

$$W(t) = \int_0^t Fv \cdot dt = \int_0^t F \cdot 2\pi RN / 60 \cdot dt = \int_0^t \pi TN / 30 \cdot dt \quad (20)$$

In the above,  $W$  is the cutting power consumption (J);  $F$  is the cutting force (N);  $v$  is the linear velocity (m/s);  $R$  is the cutting disc radius (m);  $t$  is the cutting time (s);  $T$  is the torque (n/m); and  $N$  is the rotational speed (r/min).

### 2.4.2. Experimental Factors

This study used the cutting-disc thickness, cutting-disc rotational speed, feeding speed, and edge angle as four factors with three levels in a quadratic regression orthogonal rotation combination test, with the goal of identifying the optimal parameter combination. The test factors and levels are presented in Table 2.

**Table 2.** Test factors and levels.

Level	Cutting-Disc Thickness (mm)	Cutting-Disc Rotational Speed (r·min <sup>-1</sup> )	Feeding Speed (m·s <sup>-1</sup> )	Edge Angle /(°)
−2	2	400	0.4	15
−1	3	550	0.6	20
0	4	700	0.8	25
1	5	850	1.0	30
2	6	1000	1.2	35

### 2.4.3. Cutting Power Consumption Test

A four-factor and five-level response surface analysis method was used in the test. Taking the cutting-disc thickness ( $A$ ), cutting-disc rotational speed ( $B$ ), feeding speed ( $C$ ), and edge angle ( $D$ ) as the influencing factors and the cutting power consumption ( $Y$ ) as the evaluation index, a total of 30 groups of tests were conducted. Each combination was tested three times, and the average value was used for recording the power consumption of the simulated cutting disc. The test scheme and model evaluation index results are listed in Table 3.

Table 3. Test design and results.

Serials Number	Cutting-Disc Thickness (mm)	Cutting-Disc Rotational Speed ( $\text{r}\cdot\text{min}^{-1}$ )	Feeding Speed ( $\text{m}\cdot\text{s}^{-1}$ )	Edge Angle ( $^{\circ}$ )	Cutting Power Consumption (J)
1	0	0	0	0	1.76
2	-1	1	-1	1	1.87
3	1	-1	-1	1	2.52
4	0	0	0	0	1.7
5	1	1	1	-1	1.91
6	-1	1	1	1	1.83
7	0	0	2	0	2.05
8	0	0	0	-2	1.33
9	0	0	0	0	1.76
10	1	-1	-1	-1	1.68
11	-2	0	0	0	1.23
12	-1	-1	-1	-1	1.25
13	2	0	0	0	2.46
14	0	-2	0	0	1.62
15	0	0	0	0	1.56
16	1	-1	1	-1	1.68
17	0	0	0	0	1.73
18	-1	-1	1	1	1.64
19	-1	-1	-1	1	1.45
20	0	0	0	2	2.31
21	1	1	1	1	2.56
22	1	1	-1	1	2.41
23	1	-1	1	1	2.41
24	1	1	-1	-1	1.83
25	-1	-1	1	-1	1.33
26	-1	1	1	-1	1.91
27	0	2	0	0	2.11
28	-1	1	-1	-1	1.74
29	0	0	0	0	1.87
30	0	0	-2	0	1.76

### 3. Results

#### 3.1. Single Factor Test

Figure 5 shows the influence rules of cutting-disc thickness, cutting-disc rotational speed, feeding speed and edge angle on the cutting power consumption (under the condition that the other factors are at level 0).

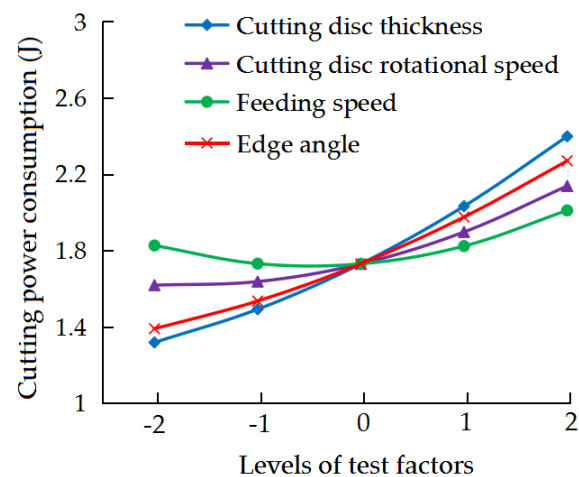


Figure 5. Influence of test factors on cutting power consumption.

The cutting power consumption decreases gradually with the increase in the cutting-disc thickness, and the decreasing trend tends to be flat. This is because when the cutting-disc thickness was large, the cutting cross-sectional area of the cutting disc increases, leading to the increase in the friction resistance of the cutting surface, which in turn leads to an increase in the cutting power consumption. However, when the cutting-disc thickness continues to increase, the changes in the stalk elasticity and plasticity were small, resulting in the relatively gentle trend of increasing cutting power consumption.

The cutting power consumption decreases slowly with the increase in the cutting-disc rotational speed, mainly because when the cutting-disc rotational speed was low, the partial elastic–plastic deformation of the castor stalk was sufficient, and the degree of deformation was much larger than that in the high-speed cutting. Thus the elastic–plastic deformation power consumption was larger, resulting in an increase in the total cutting power consumption.

The cutting power consumption decreased gradually with an increase in the edge angle because with an increase in the edge angle, the sliding effect was enhanced, the cutting ability of the blade to the castor stalk was enhanced, and the cutting resistance was reduced. Thus, the power consumption was significantly reduced.

### 3.2. Orthogonal Test Results

The test results were analyzed by quadratic regression using Design-Expert. The results of the variance analysis of the cutting power consumption  $Y$  are listed in Table 4. The regression model equations for the cutting power consumption were fitted to study the influence of each factor on the evaluation index and the influence law of the interaction.

**Table 4.** Variance analysis of regression equation.

Serials	Cutting Power Consumption $Y/J$			
	Sum of Squares	Degree of Freedom	$F$ Value	Significant Level $P$
Model	3.92	14	35.24	<0.0001 **
A	1.73	1	217.66	<0.0001 **
B	0.4	1	49.79	<0.0001 **
C	0.05	1	6.35	0.0236 *
D	1.18	1	148.53	<0.0001 **
AB	0.099	1	12.5	0.003 **
AC	$4.90 \times 10^{-3}$	1	0.62	0.4443
AD	0.31	1	39.5	<0.0001 **
BC	$2.50 \times 10^{-3}$	1	0.31	0.583
BD	0.04	1	5.04	0.0403 *
CD	$1.23 \times 10^{-3}$	1	0.15	0.7
$A^2$	0.028	1	3.46	0.0824
$B^2$	0.037	1	4.64	0.0478 *
$C^2$	0.06	1	7.52	0.0151 *
$D^2$	0.018	1	2.23	0.1559
Residual	0.12	15		
Lack of fit	0.068	10	0.66	0.7291
Pure error	0.051	5		
Total	4.04	29		

Note:  $p < 0.01$  (highly significant, \*\*);  $p < 0.05$  (significant, \*).

According to the difference analysis table, the  $p$  values of the model terms of the model are less than 0.01, indicating that the model terms are extremely significant, and the misfit terms are extremely insignificant. This indicates that the influence of each factor on each test index was extremely significant, and the model was suitable.

### 3.3. Regression Equations

For the cutting power consumption  $Y$ , all of the regression coefficients in the regression equation were adopted by the  $F$ -test at a confidence level of 0.05, and insignificant items were excluded; the regression equation was as follows:

$$Y = + 1.73 + 0.27A + 0.13B + 0.046C + 0.22D - 0.079AB + 0.14AD - 0.05BD + 0.037B^2 + 0.047C^2 \quad (21)$$

According to Equation (21) as combined with the analysis of variance table, it can be seen that the influence of each factor on the cutting power consumption was in the following order: cutting-disc thickness  $A >$  edge angle  $D >$  cutting-disc rotational speed  $B >$  feeding speed  $C$ . The primary terms  $A$ ,  $B$ , and  $D$ , and interaction terms  $AB$  and  $AD$  have extremely significant effects on the cutting power consumption. The primary term  $C$ , interaction term  $BD$ , and quadratic terms  $B^2$  and  $C^2$  have significant effects on the cutting power consumption.

## 4. Discussion

### 4.1. Analysis of the Influence of Each Factor on the Performance Index

The influences of interaction factors on the evaluation index were fixed at the intermediate level, and the interaction influences of the other two factors on the evaluation index were analyzed. The influences of the cutting-disc thickness, cutting-disc rotational speed, feeding speed, and edge angle on the evaluation index were analyzed using a response surface diagram and contour map.

Figure 6a shows the response surface diagram of the interaction between the cutting-disc thickness and edge angle on the cutting power consumption when the cutting-disc rotational speed and feeding speed are at an intermediate level. It can be seen from Figure 6a that with an increase in the cutting-disc thickness, the cutting power consumption clearly shows a gradual upward trend. With an increase in the edge angle, the cutting power consumption increases significantly. This is because with an increase in the cutting-disc thickness, the extrusion stalk fiber tissue has an elastic–plastic recovery to cutting disc, leading to a higher cutting surface resistance and higher cutting power consumption. Under the same cutting conditions, the smaller the blade radius, the greater the local stress on the stalk. The smaller the blade angle, the smaller the blade radius; this makes it easier for the blade to break the physical structure, thereby reducing the cutting power consumption.

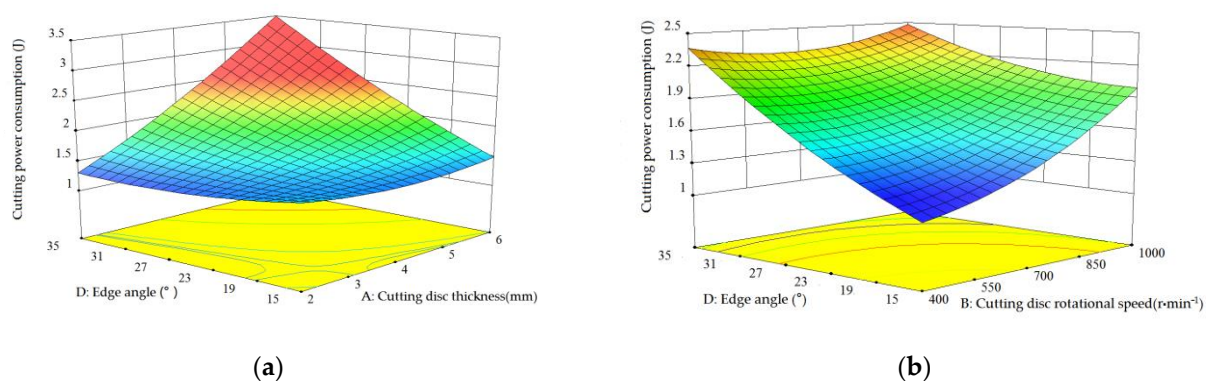


**Figure 6.** Influence of interactive factors on cutting power consumption.

The response surface diagram of the interaction between the cutting-disc rotational speed and edge angle on the cutting power consumption when the cutting-disc thickness and feeding speed are at the intermediate level is shown in Figure 6b. With an increase in the cutting-disc rotational speed, the cutting power consumption exhibits an upward trend and tends to be flat with an increase in the edge angle. With an increase in the rotating speed, vibration and beating of the cutting disc can easily occur. Correspondingly, the surface energy of the side affected by the elastic and plastic deformation of the stalk

increases, leading to an increase in the cutting power consumption. However, with an increase in the edge angle, the edge side squeezes the stalk, resulting in further deformation and destruction of the stalk in the cutting and the axial directions. In this case, the energy consumption increases significantly.

#### 4.2. Parameter Optimization

To obtain the minimum cutting power consumption of the waved-type cutting disc, the optimization module in Design-Expert was used to optimize and solve the regression model. Its constraints were as follows:

$$\begin{cases} \min Y(A, B, C, D) \\ 2 \leq A \leq 6 \\ 400 \leq B \leq 1000 \\ 0.4 \leq C \leq 1.2 \\ 15 \leq D \leq 35 \end{cases} \quad (22)$$

A set of optimal solutions was obtained by optimizing the objective function, and the optimal combination of cutting operation parameters was as follows: cutting-disc thickness of 3 mm, cutting-disc rotational speed of 550 r/min, feeding speed of 0.6 m/s, and edge angle of 20°. Under these conditions, the cutting power consumption is 1.20375 J.

#### 4.3. Verification Results

To test the correctness of the optimal combination of cutting-disc parameters obtained with the response surface method, experiments were repeated five times under these conditions, as shown in Table 5.

**Table 5.** Verification test results.

Items	Predicted Value	Test Value 1	Test Value 2	Test Value 3	Test Value 4	Test Value 5
Cutting power consumption/J	1.20375	1.23	1.21	1.25	1.20	1.21

The average cutting power consumption obtained was 1.22 J, i.e., less than 1% different from the predicted value of the model. This indicated that there is a good fit between the test values and the predicted values. The experimental effect after optimizing the parameters was good. This proved that the response surface method was reliable and effective in optimizing the operating parameters of the cutting-disc device.

#### 4.4. Discussion

The operation quality of castor-harvesting equipment is of paramount importance for the development of the castor industry. At present, studies related to castor harvest mainly focus on the characteristics of castor fruits and the shelling machinery, and there are few studies on the cutting resistance and power consumption of castor-cutting devices.

This research provided experimental innovations, but there are some limitations. Because of subjective and objective factors such as time and conditions, the experimental research on the mechanical properties of castor plants was lacking. Next, this study only carried out castor cutting harvesting experiments on selected varieties; however, in China, there are many castor varieties, with very different physical characteristics. Therefore, the adaptability of the equipment needs to be verified for different varieties. In addition, this paper is an experimental study based on the test bench, and does not consider the influence of the actual field operating conditions on the power consumption. It is necessary to further study the cutting resistance and power consumption under the actual field operating conditions in future research.

## 5. Conclusions

To reduce of the cutting resistance and power consumption in the castor-cutting harvest process, this study carried out a theoretical analysis of the cutting process using a castor-cutting disc; experiments were conducted based on orthogonal rotation combination of multiple factors and simulations of the cutting-disc thickness, cutting-disc rotational speed, feeding speed, and edge angle. The influences on the cutting power consumption and parameters were optimized using the response surface method, and the optimal parameter combination was determined from the experiments.

The orthogonal rotation combination test results showed that the cutting-disc thickness, cutting-disc rotational speed and edge angle had highly significant impacts on the cutting power consumption, and feeding speed had a significant impact on the cutting power consumption. The optimal parameter combination was as follows: cutting-disc thickness of 3 mm, cutting-disc rotational speed of 550 r/min, feeding speed of 0.6 m/s, and edge angle of 20°. Under these conditions, the cutting power consumption was 1.20375 J. The results of this study can provide a reference for the further optimization of the structural parameters of the castor-cutting disc.

**Author Contributions:** Conceptualization, T.W., F.K. and L.S.; methodology, F.K., T.W. and Y.S.; software, Q.X. and Y.S.; validation, L.S. and C.C.; writing—original draft preparation, F.K., T.W. and Q.X.; writing—review and editing, L.S., Y.S. and C.C. All authors have read and agreed to the published version of the manuscript.

**Funding:** This research was funded by the Agricultural Science and Technology Innovation Program of Chinese Academy of Agricultural Sciences (CAAS-ASTIP-31-NIAM-05); Central Public-Interest Scientific Institution Basal Research Fund (S202111-02).

**Institutional Review Board Statement:** Not applicable.

**Data Availability Statement:** Not applicable.

**Acknowledgments:** We greatly appreciate the careful and precise reviews by the anonymous reviewers and editors.

**Conflicts of Interest:** The authors declare no conflict of interest.

## References

1. Mensah, M.B.; Awudza, J.A.M.; O'Brien, P. Castor oil: A suitable green source of capping agent for nanoparticle syntheses and facile surface functionalization. *R. Soc. Open Sci.* **2018**, *5*, 180824. [CrossRef]
2. Pari, L.; Suardi, A.; Stefanoni, W.; Latterini, F.; Palmieri, N. Environmental and economic assessment of castor oil supply Chain: A case study. *Sustainability* **2020**, *12*, 6339. [CrossRef]
3. Severino, L.S.; Auld, D.L.; Baldanzi, M.; Cândido, M.J.D.; Chen, G.; Crosby, W.; Tan, D.; He, X.; Lakshamma, P.; Lavanya, C.; et al. A review on the challenges for increased production of castor. *Agron. J.* **2012**, *104*, 853–880. [CrossRef]
4. Anjani, K.A.K. A re-evaluation of castor (*Ricinus communis* L.) as a crop plant. *CAB Rev. Perspect. Agric. Veter. Sci. Nutr. Nat. Resour.* **2014**, *9*, 1–21. [CrossRef]
5. Kong, F.T.; Wu, T.; Shi, L.; Zhang, Y.T.; Chen, C.L.; Sun, Y.F. Research status and development prospect of ricinus communis harvester. *J. Chin. Agric. Mech.* **2019**, *40*, 32–36. [CrossRef]
6. Pari, L.; Latterini, F.; Stefanoni, W. Herbaceous oil crops, a review on mechanical harvesting state of the art. *Agriculture* **2020**, *10*, 309. [CrossRef]
7. Wu, T.; Kong, F.T.; Shi, L.; Chen, C.L.; Sun, Y.F.; Xie, Q. Analysis of the development status of Ricinus communis production technology. *J. Chin. Agric. Mech.* **2019**, *40*, 77–81. [CrossRef]
8. Claas Ohg Beschraenkt Haftende Offene Handelsgesellschaft, Centre National Du Machinisme Agricole, Du Genie Rural, Des Eaux Et Des Forets (CEMAGREF). Self-Propelled Harvester for Harvesting Delicate Crops Und as Castor-Oil Seeds. E.P. Patent 19940250172, 11 January 1995.
9. Deere & Company. Header for Harvesting Castor Beans. U.S. Patent 19590831646, 23 April 1962.
10. Li, C.H.; Liu, C.C.; Zhuang, W.H.; Zhu, Z.W. The structural design and motion simulation of the comb-type castor picking system. *J. Mach. Des. Manuf.* **2016**, *5*, 95–98. [CrossRef]
11. Wu, C.F.; Chen, W.C.; Sheng, C.T. Study on the harvester development of ricinus communis. *J. Agric. Fore.* **2013**, *62*, 33–44. Available online: <https://ir.lib.nchu.edu.tw/handle/11455/93621> (accessed on 6 December 2017).
12. Liu, L.; Wu, T.; Kong, F.T.; Sun, Y.F.; Chen, C.L.; Xie, Q.; Shi, L. Optimized design and experiment of the picking mechanism for brush-roller castor harvesters. *Trans. Chin. Soc. Agric. Eng.* **2021**, *37*, 19–29.

13. Bai, J.B. *The Design of Small-Sized Castor Harvester and Cutting Device*; Shenyang Agricultural University: Shenyang, China, 2019. [[CrossRef](#)]
14. Song, Z.H.; Song, H.L.; Yan, Y.F.; Li, Y.D.; Gao, T.H.; Li, F.D. Optimizing design on knife section of reciprocating cutter bars for harvesting cotton stalk. *Trans. Chin. Soc. Agric. Eng.* **2016**, *32*, 42–49.
15. Guo, Q.; Zhang, X.L.; Xu, Y.F.; Li, P.P.; Chen, C.; Wu, S. Design and experiment of cutting blade for cane straw. *Trans. Chin. Soc. Agric. Eng.* **2014**, *30*, 47–53.
16. Chen, Z.G.; Wang, D.F.; Li, L.J.; Shan, R.X. Experiment on tensile and shearing characteristics of rind of corn stalk. *Trans. Chin. Soc. Agric. Eng.* **2012**, *28*, 59–65.
17. Ugwu, K.C.; Egbuagu, O.M.; Omoruyi, A. Determination of some mechanical and aerodynamic properties of castor fruits and seeds. *Int. J. Sci. Eng. Res.* **2015**, *6*, 659–666.
18. Cao, Y.H.; Li, C.Y.; Zhang, Z.X.; Qing, Y.M.; Yao, L.L. Improvement design and test to key components of castor capsule hulling device. *Trans. Chin. Soc. Agric. Eng.* **2012**, *28*, 16–22.
19. Lorestani, A.N.; Jalilantabar, F.; Gholami, R. Physical and mechanical properties of castor seed. *Qual. Assur. Saf. Crop. Foods* **2012**, *4*, e29–e32. [[CrossRef](#)]
20. Wang, J.W.; Guan, R.; Gao, P.X.; Zhou, W.Q.; Tang, H. Design and Experiment of Single Disc to Top Cutting Device for Carrot Combine Harvester. *Trans. Chin. Soc. Agric. Mach.* **2020**, *51*, 74–81. [[CrossRef](#)]
21. Maughan, J.D.; Mathanker, S.K.; Fehrenbacher, B.M.; Hansen, A.C. Impact of cutting speed and blade configuration on energy requirement for miscanthus harvesting. *Appl. Eng. Agric.* **2014**, *30*, 137–142. [[CrossRef](#)]
22. Orłowski, K.; Ochrymiuk, T. A newly-developed model for predicting cutting power during wood sawing with circular saw blades. *Maderas Cienc. Tecnol.* **2017**, *19*, 149–162. [[CrossRef](#)]
23. Li, C.; Zhang, H.; Wang, Q.; Chen, Z. Influencing factors of cutting force for apple tree branch pruning. *Agriculture* **2022**, *12*, 312. [[CrossRef](#)]
24. Zhang, B.; Liu, H.; Huang, J.; Tian, K.; Shen, C.; Li, X.; Wang, X. Ramie field distribution model and miss cutting rate prediction based on the statistical analysis. *Agriculture* **2022**, *12*, 651. [[CrossRef](#)]
25. Song, S.Y.; Zhou, H.P.; Xu, L.Y.; Jia, Z.C.; Hu, G.M. Cutting mechanical properties of sisal leaves under rotary impact cutting. *Ind. Crops Prod.* **2022**, *182*, 114856. [[CrossRef](#)]
26. Kong, F.T.; Wang, D.F.; Shi, L.; Wu, T.; Chen, C.L.; Sun, Y.F.; Xie, Q. Design and experiment of disc-cutting picking device of castor. *Trans. Chin. Soc. Agric. Eng.* **2021**, *37*, 1–9. [[CrossRef](#)]